

Synthesis and characterization of cardanol containing tetra-functional fluorene-based benzoxazine resin having two different oxazine ring structures

Yu-Peng Chen^a, Xuan-Yu He^{a,b}, Abdul Qadeer Dayo^{a,d}, Jun-Yi Wang^a, Wen-bin Liu^{a,*}, Jun Wang^{a,**}, Tao Tang^{c,***}

^a Key Laboratory of Superlight Material and Surface Technology of Ministry of Education, College of Materials Science and Chemical Engineering, Harbin Engineering University, Harbin, 150001, China

^b Xi'an Aerospace Composites Research Institute, Xi'an, 710025, China

^c State Key Laboratory of Polymer Physics and Chemistry, Changchun Institute of Applied Chemistry, Chinese Academy of Science, Changchun, 130022, PR China

^d Department of Chemical Engineering, Balochistan University of Information Technology, Engineering and Management Sciences, Quetta, 87300, Pakistan

HIGHLIGHTS

- Synthesis of a new cardanol containing tetra-functional benzoxazine monomer (t-BF-a-c).
- The t-BF-a-c monomer showed good processability.
- The poly (t-BF-a-c) showed much better thermal properties than the other bi-functional cardanol based polybenzoxazines.

ARTICLE INFO

Keywords:

Tetra-functional benzoxazine
Cardanol
Thermomechanical properties

ABSTRACT

A new cardanol containing tetra-functional fluorene-based (t-BF-a-c) benzoxazine resins has been successfully synthesized via two-stage Mannich condensation reaction. The monomer contains simultaneous diamine- and bisphenol-type oxazine rings. The FTIR, ¹H and ¹³C NMR tests were performed to confirm the structure of intermediates and t-BF-a-c benzoxazine. The rheological properties and curing behavior of the resin and thermal and thermomechanical properties of the corresponding polymer (poly (t-BF-a-c)) were evaluated by rheometer, differential scanning calorimeter, thermogravimetric analysis, and dynamic mechanical analyzer. The synthesized benzoxazine resin displays good processability and wide process window due to the incorporation of cardanol. Poly (t-BF-a-c) exhibits much higher glass transition temperature (373 °C) than corresponding bi-functional polybenzoxazines and better thermal stability than mono- and bi-functional cardanol-based polybenzoxazines. With the introduction of the flexible long alkyl chain of cardanol, the brittleness of fluorene-based polybenzoxazine is greatly modified without sacrificing thermal properties of the polymer.

1. Introduction

Since the start of the 21st century, the growing environmental concerns and the rapid fluctuation in the petrochemical prices diverted the attention of researchers towards the synthesis of monomers and polymers from bio-based resources [1,2]. The cellulose, lignin, tannins, starch, castor oil, cashew nut shell oil, chitin, and chitosan are the most widely used bio-based materials [3]. The cardanol is a pale yellow

phenolic oil obtained as a byproduct from the cashew nut processing industry. The cardanol having a long alkyl side chain has attracted the attention of researchers working on the high performance polymers. A variety of high performance polymers have been synthesized from the cardanol, which includes polybenzoxazine (PBz), polynaphthols, phthalonitrile, alkyds, melamines, polyesters, etc, are successfully synthesized from the cardanol [4]. However, the cardanol based polymers exhibit higher flexibility as compared to the simple phenol based

* Corresponding author.

** Corresponding author.

*** Corresponding author.

E-mail addresses: liuwenbin@hrbeu.edu.cn (W.-b. Liu), wj6267@hrbeu.edu.cn (J. Wang), ttang@ciac.jl.cn (T. Tang).

polymers due to internal plasticization due to the presence of long alkyl side-chain, this chain also reduces the thermal and thermomechanical properties of the polymers [5].

The PBz resins provide some outstanding characteristics such as no generation of by-products, excellent flame retardancy and higher thermal stability, near zero shrinkage upon polymerization, and low moisture absorption. The extraordinary molecular design flexibility of PBz resins as compared to other polymers and brings a wide range of properties [6–9]. The synthesis of fluorene-based polymers attracted the researchers due to the reduced segmental activity, and significant enhancements in the glass transition temperature (T_g) and thermal stabilities. Several types of fluorene-based high performance polymers are successfully synthesized such as PBz, polyimides, poly (ether imide), and epoxy [10–19]. However, the low toughness and high fragility of the fluorenyl containing polymers limit their further application. In our previous studies, we introduced the aryl ether and aryl ester in the monomer structure to improve the toughness of the polybenzoxazines [20,21].

In the current study, keeping in view the higher fragility of the fluorenyl containing polymers and flexibility of the cardanol based polymers, we successfully synthesized a new cardanol containing tetrafunctional fluorene-based benzoxazine monomer (*t-BF-a-c*). A single molecule of the monomer contains diamine- and bisphenol-type oxazine rings. The detailed synthesis, polymerization behavior, and properties of poly (*t-BF-a-c*) are investigated.

2. Experimental

2.1. Materials

Shanghai Jingchun Reagent Co., Ltd. Shanghai, China supplied the 2,7-Dihydroxy-9-fluorenone, *p*-formaldehyde, trifluoroacetic anhydride, 4-chlorobenzene, sodium borohydride, and methyl sulfonic acid. Cardanol, distilled technical grade, was kindly obtained from Shandong Haobo Co. Ltd. Shandong, China. Aniline and all the solvents used in the current study were supplied by Tianjin Kermel Chemical Reagent Co., Ltd. Tianjin, China. All the materials were used without further purification.

2.2. Synthesis of monomer

The condensation reaction of bisphenol or diamine with formaldehyde and primary amine or phenol produced the benzoxazine monomer as a product. In the current study, the simultaneous presence of bisphenol and diamine functional groups in 9,9-bis(4-aminophenyl)-2,7-dihydroxyindole (*b-AHF*) (intermediate monomer) make it difficult to obtain a monomer with two different oxazine ring structure. Therefore, we utilize a two-stage Mannich condensation reaction to synthesize *t-BF-a-c* benzoxazine resin (Scheme 1). Firstly, diamine in the *b-AHF* was protected by using the trifluoroacetic anhydride to afford amine-protected 9,9-bis(4-trifluoroacetamidophenyl)-2,7-dihydroxy-fluorene (*b-PAHF*). Later, the amine-protected biphenol-type benzoxazine (*b-pABF-a*) was obtained via the first Mannich condensation reaction of *b-pAHF* with aniline and paraformaldehyde. Subsequently, *b-pABF-a* was deprotected with sodium borohydride in ethyl acetate/ethanol solution to liberate amine. Finally, the *t-BF-a-c* benzoxazine resin was prepared by the second Mannich condensation reaction of amine-liberated biphenol-type benzoxazine (*b-ABF-a*) with paraformaldehyde and cardanol. The details of each step are provided below, Scheme 1 shows the followed synthesis route.

2.2.1. Preparation of *b-AHF*

The 2,7-dihydroxy-9-fluorenone and aniline were reacted by following the method as described by Wang et al.; [22]. The yield of a yellow powder (compound 1) was 86%. ^1H NMR (500 MHz, $\text{DMSO}-d_6$, ppm): 9.24 (s, 2H, -OH), 6.40–7.45 (m, 14H, Ar-H), 4.93 (s, 4H, -NH₂).

FTIR (KBr, cm^{-1}): ν = 3375 (N–H stretching), 3308 (–OH stretching), 1610 and 1445 (aromatic stretching vibration), 1484 (1,2,4-trisubstituted characteristic absorption), 1182 (C–N asymmetric stretching).

2.2.2. Preparation of *b-PAHF*

Compound 1 (19.0 g, 0.05 mol) and THF (200 mL) were added into a 250 mL round flask and cooled for 30 min in an ice bath. Afterward, trifluoroacetic anhydride (23.1 g, 0.11 mol) was added dropwise in 30 min during the mixture stirring; later, the mixture was stirred for 2 h in an ice bath. The solvent was removed by a rotary evaporator, followed by dissolving the residue in ethyl acetate. The solution was washed five times with saturated aqueous Na_2CO_3 solution and three times with distilled water. The solution was dried with sodium sulfate, filtered, and concentrated under vacuum. The product was precipitated in hexane (500 mL), filtered, and overnight dried under vacuum. The yield of yellowish powder (compound 2) was 92%. ^1H NMR (500 MHz, $\text{DMSO}-d_6$, ppm): 11.31 (s, 2H, -NH), 9.44 (s, 2H, -OH), 6.71–7.58 (m, 14H, Ar-H). IR (KBr, cm^{-1}): ν = 3600–3100 (N–H and O–H stretching overlap), 1704 (C=O stretching).

2.2.3. Preparation of *b-PABF-a*

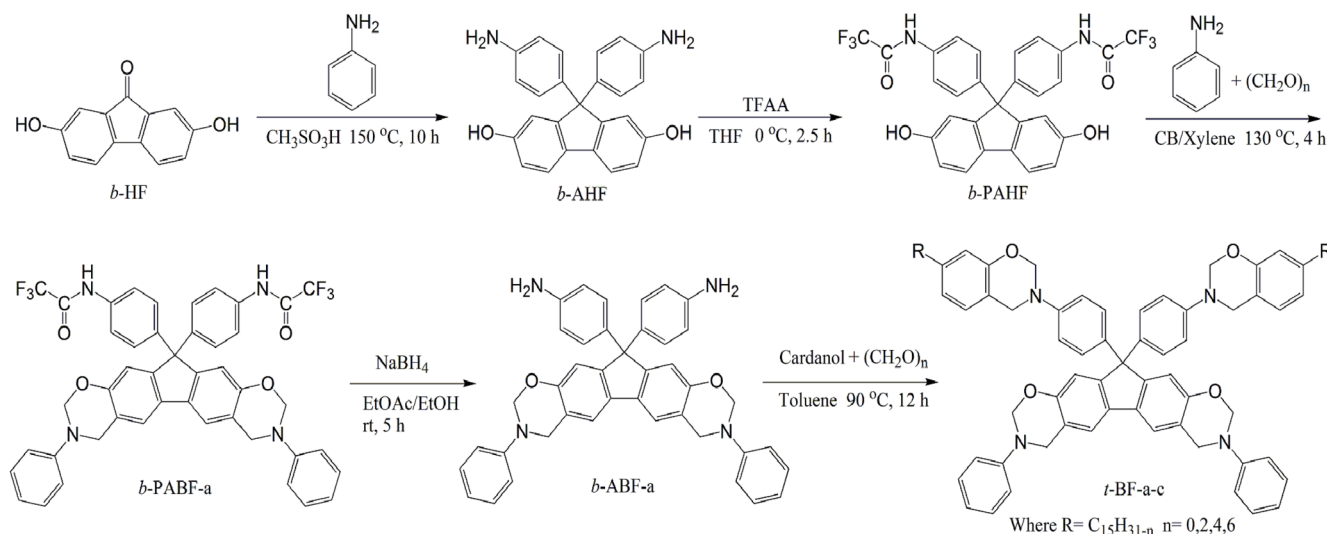
A 100 mL neck round-bottomed flask was connected with reflux condenser, thermometer, and magnetic stirrer, and compound 2 (5.72 g, 0.01 mol), aniline (1.86 g, 0.02 mol), *p*-formaldehyde (1.20 g, 0.04 mol) and 30 mL of chlorobenzene/xylenes (1:1) were added and mixed for 4 h at 130 °C, and cooled to room temperature. Later, the hexane was mixed in the cooled mixture, and produced precipitated were separated by the filtration. The yellowish powder was thoroughly washed with ethanol and vacuum dried at 60 °C for one night. Afterward, the crude product was dissolved in dichloromethane (100 mL), and three times washed with 100 mL each of 5 wt % aqueous Na_2CO_3 solution and water. The white powder (compound 3, with 83% yield) was obtained after the solution drying over anhydrous sodium sulfate, followed by evaporation of the solvent under vacuum. ^1H NMR (500 MHz, $\text{DMSO}-d_6$, ppm): 11.24 (s, 2H, -NH), 6.73–7.53 (m, 22H, Ar-H), 4.74 (s, 4H, Ar-CH₂-N), 5.44 (s, 4H, O-CH₂-N). IR (KBr, cm^{-1}): ν = 3297 (N–H stretching), 1711 (carbonyl stretching), 1478 (stretching of 1,2,4,5-tetrasubstituted benzene ring), 1244 (asymmetric stretching of C–O–C), 950 (the oxazine ring stretching mode with a minor contribution of CH out-of-plane bending).

2.2.4. Preparation of *b-ABF-a*

Compound 3 (8.06 g, 0.01 mol) was dissolved in a 200 mL mixture of methanol/ethyl acetate at a ratio of 1:100 in a 500 mL flask. The NaBH_4 (3.78 g, 0.10 mol) was added in the solution, and the nitrogen atmosphere was adjusted and stirred for 5 h at room temperature. Later, the mixture was three times washed with brine and water. After that, ethyl acetate was withdrawn by using a rotary evaporator, and vacuum dried at 60 °C for 24 h. The yield of the final product (compound 4) was 71%. ^1H NMR (500 MHz, $\text{DMSO}-d_6$, ppm): 4.70 (s, 4H, Ar-CH₂-N), 4.89 (s, NH₂), 5.41 (s, 4H, O-CH₂-N), 6.35–7.41 (22H Ar). IR (KBr, cm^{-1}): ν = 3363 (N–H stretching), 1478 (stretching of 1,2,4,5-tetrasubstituted benzene ring), 1225 (asymmetric stretching of C–O–C), 1182 (asymmetric stretching of C–N–C), 941 (the oxazine ring stretching mode with minor contribution of CH out-of-plane bending).

2.2.5. Preparation of *t-BF-a-c*

In a 250 mL flask, compound 4 (3.07 g, 0.005 mol), cardanol (3.05 g, 0.01 mol), *p*-formaldehyde (0.90 g, 0.03 mol) and 20 mL of toluene were manually mixed till the uniformity of solution. Later, the solution was stirred for 12 h at 90 °C and cooled down to room temperature. Afterward, the hexane was poured in the mixture, and the product (yellowish precipitates) were obtained after the filtration and 24 h vacuum drying, the yield of product was 79%. ^1H NMR (500 MHz, CDCl_3-d_1 , ppm): 6.48–7.45 (m, 28H, Ar-H), 5.32–5.40 (vinyl double bond), 5.33 (s, 4H, O-CH₂-N), 5.25 (s, 4H, O-CH₂-N), 4.69 (s, 4H,

Scheme 1. Synthetic route of *t*-BF-*a*-*c* benzoxazine resin.

Ar-CH₂-N), 4.52 (s, 4H, Ar-CH₂-N). FTIR (KBr, cm⁻¹): 1654, 992 (C=C stretching), 1367 (CH₂ wagging), 1214, 1261 (C-O-C asymmetric stretching), 1110–1190 (C-N-C asymmetric stretching), 1032, 1073 (C-O-C symmetric stretching), 929–962 (C-H out-of-plane bending), 919 (the oxazine ring stretching mode with minor contribution of CH out-of-plane bending).

2.3. Curing of benzoxazine monomers

The *t*-BF-*a*-*c* benzoxazine resin was polymerized without the added initiator or catalyst. The monomer was isothermally cured in an air-circulating oven by keeping them at 150, 180, and 210 °C for 2 h at each stage. The polymer was post-cured for 1 h at 240 °C in an air-circulating oven.

2.4. Characterization

A PerkinElmer Spectrum-100 spectrometer was used to record the Fourier transform infrared (FTIR) spectra in the range of 4000–500 cm⁻¹, at a 4 cm⁻¹ resolution, after averaging two scans. The sample (monomers or cured) was blended with KBr powder, a thin KBr pellet was prepared, and the spectrum of the pellet was recorded in the presence of deuterated triglycine sulfate (DTGS) detector. The Bruker AVANCE-500 NMR spectrometer was used to test the ¹H and ¹³C NMR. The average number of transients for ¹H and ¹³C NMR is 32 and 1024, respectively. The tests were performed after dissolving the samples in deuterated DMSO (DMSO-*d*₆) and CDCl₃, while tetramethylsilane (TMS) was used as an internal standard. A TA Q200 differential scanning calorimeter was used to evaluate the differential scanning calorimetry (DSC) measurements at a heating rate of 20 °C/min, from 30 to 350 °C, under a constant (50 mL/min) flow of nitrogen gas. Prior to the samples testing, the DSC machine was calibrated with a high-purity indium standard. A 5 mg of sample was weighed into a hermetic aluminum sample pan at room temperature (24 °C), which was then sealed, and tested immediately. The TA Instruments AR-2000ex Rheology was used to evaluate the dynamic rheological measurements. The tests were performed on a 6.283 rad/s angular frequency and 4 °C/min heating rates. Thermal stability of the polymer was evaluated by analyzing the thermogravimetric analysis (TGA) under a nitrogen atmosphere (50 mL/min), performed on a TA Instruments Q50 from 25 to 820 °C at a 20 °C/min heating rate. The thermomechanical properties of the polymer were obtained by evaluating a rectangular (35 × 5 × 2 mm³) polybenzoxazine sample on a dynamic mechanical analyzer (DMA) TA-Q800, USA. The sample was loaded in single cantilever mode, and

tested at 3 °C/min heating rate from 30 to 390 °C, with a 1 Hz frequency of air atmosphere.

3. Results and discussion

3.1. Benzoxazine monomers structure

The ¹H NMR spectra intermediate compounds (*b*-AHF, *b*-pAHF, *b*-pABF-*a*, and *b*-ABF-*a*) and final *t*-BF-*a*-*c* benzoxazine resin are plotted as Fig. 1. We can easily observe from Fig. 1(A) that the -OH protons shift from 9.26 to 9.44 ppm, and the -NH₂ protons located at 4.92 ppm disappear before and after amine protection for *b*-AHF. The new protons peak of CF₃CONH- at 11.24 ppm was observed. After the first Mannich condensation and amine deprotection, the typical resonances of bisphenol-type benzoxazine and deprotected amine groups appear at 4.70, 5.41, and 4.89 ppm, respectively. The methylene protons of diamine-type benzoxazine were located (at 4.52 and 5.25 ppm) after the second Mannich condensation reaction (Fig. 1(B)). The disappearance of the deprotected amine group peak confirms the formation of two different kinds of oxazine rings connected with phenyl and fluorene rings, respectively. The peaks at 5.36 and 5.43 ppm, and 4.97–5.06 and 5.78–5.81 ppm weak peaks can be ascribed to the -CH=, CH₂=CH-, and -CH=CH₂ protons of cardanol, respectively. These resonances are in agreement to the long alkyl side chain of cardanol [23]. In addition, the integral ratio of the methylene protons is nearly 1:1:1:1, indicating that the *t*-BF-*a*-*c* benzoxazine resin is successfully synthesized.

The ¹³C NMR spectra intermediate monomers (*b*-ABF-*a* and *b*-pABF-*a*) and final *t*-BF-*a*-*c* benzoxazine monomers are displayed in Fig. 2. The carbon atom resonances of O-CH₂-N and Ar-CH₂-N oxazine ring were observed at 49.27–50.55 and 78.84–79.43 ppm, respectively. In particular, there were four kinds of oxazine rings carbon atom resonances in *t*-BF-*a*-*c* benzoxazine monomer backbone, bisphenol-type oxazine rings (50.55 and 79.42 ppm) and diamine-type oxazine rings (50.11 and 79.32 ppm). The quaternary carbon atom of the fluorene ring was recorded at around 63.8 ppm. The *b*-pABF-*a* intermediate showed multiple new peaks around 154.6 and 153.44 ppm, these peaks can be attributed to the resonance of carbon atom of -CF₃ and -CO-, respectively.

The FTIR spectrum of *t*-BF-*a*-*c* benzoxazine monomer (Fig. 3) showed the out-of-plane bending of C-H at 962 and 929 cm⁻¹, which can be corresponded to the phenyl and fluorene with an oxazine ring attached, respectively. The asymmetric stretching of C-O-C (1214 and 1261 cm⁻¹) and C-N-C (1110–1190 cm⁻¹), symmetric stretching of C-O-C (1073 and 1032 cm⁻¹), and CH₂ wagging (1367 cm⁻¹) of

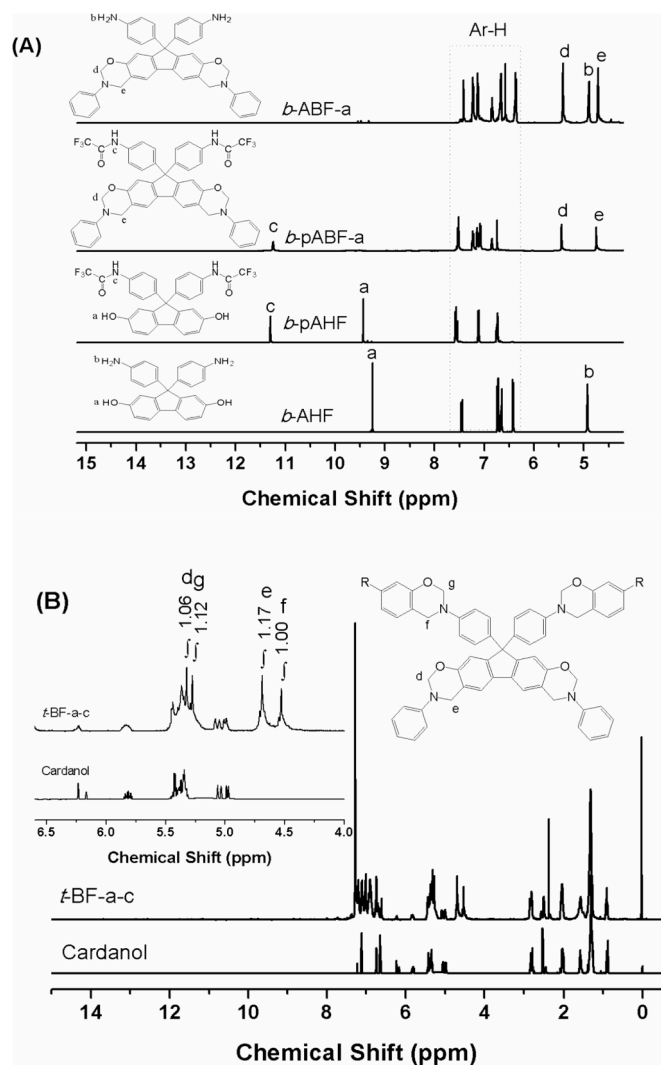


Fig. 1. ¹H NMR spectra of *t*-BF-*a*-*c* benzoxazine intermediates (A) and final monomer (B).

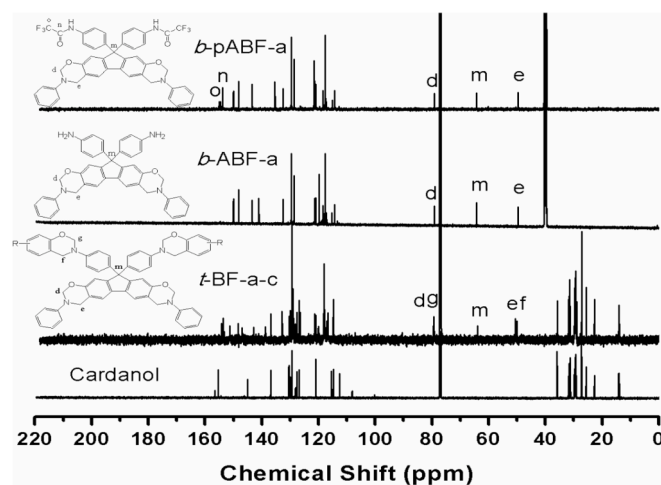


Fig. 2. ¹³C NMR spectra of novel *t*-BF-*a*-*c* benzoxazine monomer and their intermediates.

oxazine ring connected with benzene and fluorene, respectively, are also observed. Additionally, the C=C stretching and out-of-plane deformation of =C-H in the unsaturated moiety of cardanol were observed at 1654, and 992 cm⁻¹ the characteristic absorption,

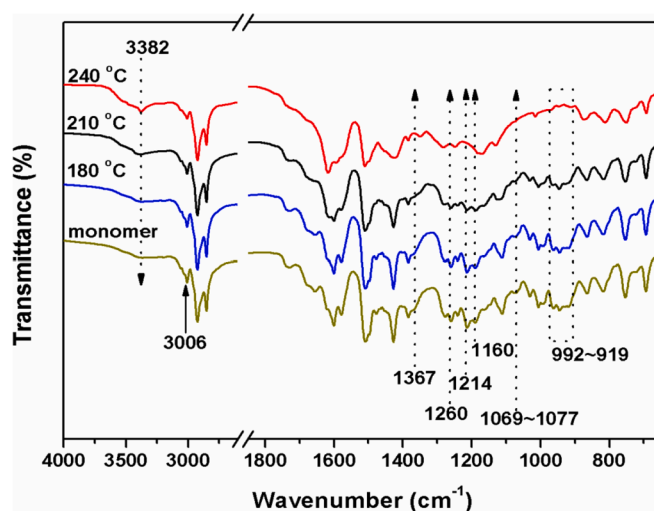


Fig. 3. The FTIR spectra of *t*-BF-*a*-*c* benzoxazine monomer after different isothermal curing stages, and poly (*t*-BF-*a*-*c*).

respectively. These FTIR, ¹H and ¹³C NMR spectra indicate the successful synthesis of targeted cardanol containing tetra-functional fluorene-based benzoxazine monomer.

3.2. Polymerization behavior of benzoxazine monomer

The polymerization behavior of the synthesized *t*-BF-*a*-*c* benzoxazine monomer was investigated by FTIR and DSC. The FTIR spectra of neat *t*-BF-*a*-*c* benzoxazine monomer before and after cumulative curing at 180, 210, and 240 °C are plotted as Fig. 3. The absorption band intensities ascribed to oxazine ring, symmetric stretching of C-O-C, CH₂ wagging, asymmetric stretching of C-N-C and C-O-C, and out-of-plane bending of C-H gradually decrease as the curing temperature increases and curing proceeds. The similar phenomena were also recorded for the olefinic bond peaks due to the C=C stretching and out-of-plane deformation of =C-H, and completely disappear on the completion of the curing process. These results indicate that high-temperature ring-opening polymerization can further carry out the cross-linking reaction and increase the cross-linking density of polybenzoxazine. Meanwhile, the FTIR spectrum of poly(*t*-BF-*a*-*c*) confirmed the hydrogen bonding (intramolecular and intermolecular) by the broad peak at 3382 cm⁻¹ with a shoulder. The hydrogen bonding was recorded due to the ring-opening of benzoxazine, the shoulder confirmed the overlapping in the crosslinked network structure of polybenzoxazine [24].

The dynamic DSC plot of the *t*-BF-*a*-*c* benzoxazine monomer before and after each curing stage were evaluated, produced curves are illustrated in Fig. 4. The *t*-BF-*a*-*c* benzoxazine monomer only exhibits an exothermal peak at 277 °C with 121.4 J/g of enthalpy value. The exothermic peak was slightly wide as compared to the traditional benzoxazine monomers; this can be due to the overlap of oxazine ring-opening and addition polymerization of double bonds in the alkyl side chain of cardanol. In addition, the small value (121.4 J/g) for the heat of polymerization was observed due to the dilution effect of cardanol having long alkyl chains in the structure [25]. In addition to this, the *t*-BF-*a*-*c* benzoxazine monomer does not show the very wide peak or shoulders, even though the single molecule contains two different oxazine rings as recorded for the other fluorene-based benzoxazine [22], may be due to the addition of alkyl side chain of cardanol. This confirms that the steric hindrance was not observed during the polymerization.

Moreover, from the produced curves we can easily observe that the exothermic peak temperature moves to a higher temperature as the curing process moves on from one to another curing stage. This can be dedicated to the formed network structures and increased curing degree, which reduced the system viscosity, polymerization rate, and

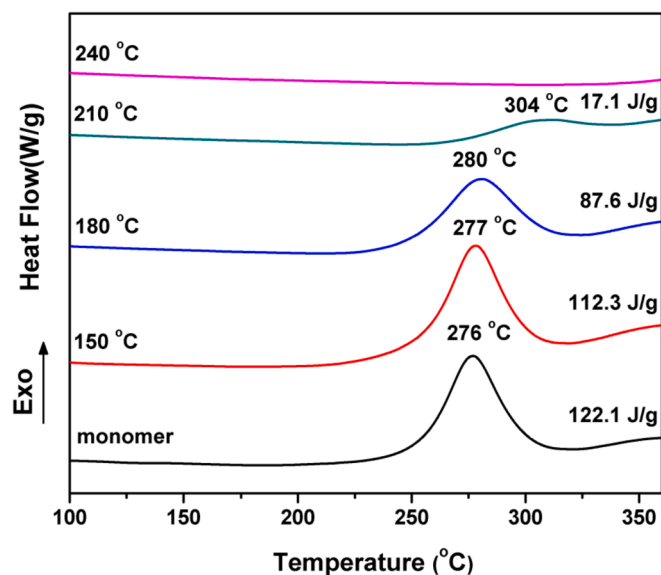


Fig. 4. The DSC curves of neat *t*-BF-*a*-*c* benzoxazine monomer after different isothermal curing stages.

activity of the functional group in the system. In addition to these, the reactivity of functional groups can be increased by increasing the curing temperature, which ultimately completes the curing of the monomer [20,21]. After the complete curing procedure, DSC curves did not show any exothermic peak, and the T_g was not observed in the studied temperature range.

The rheological properties provide a basic understanding of the polymer's processability because it produces the melting point, gel point, and processing window of the monomer. The melting point corresponds to the conversion of the solid to liquid, while, the gel point corresponds to the conversion of the liquid to the solid (conversion of the monomers to polymer). The processing window is very useful for the polymer compounding or processing, it is the temperature range in between melting point and gel point [26,27].

The viscoelastic response of *t*-BF-*a*-*c* benzoxazine resin against the temperature is plotted as Fig. 5. For keeping the consistency in the study, the liquefying and gel point temperatures value of *t*-BF-*a*-*c* benzoxazine monomer was defined at 1000 Pa s viscosity, the corresponding recorded values were 116 and 176 °C. This shows a processing window of 60 °C, which is good enough for the processing of polymer.

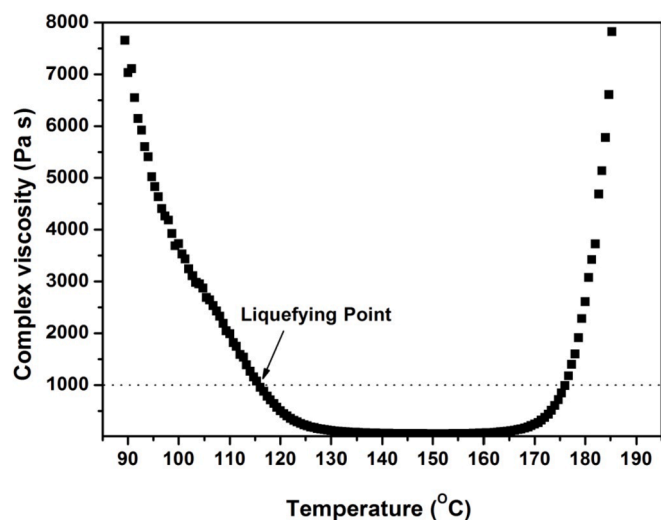


Fig. 5. The relationship between dynamic viscosity and temperature of *t*-BF-*a*-*c* monomer.

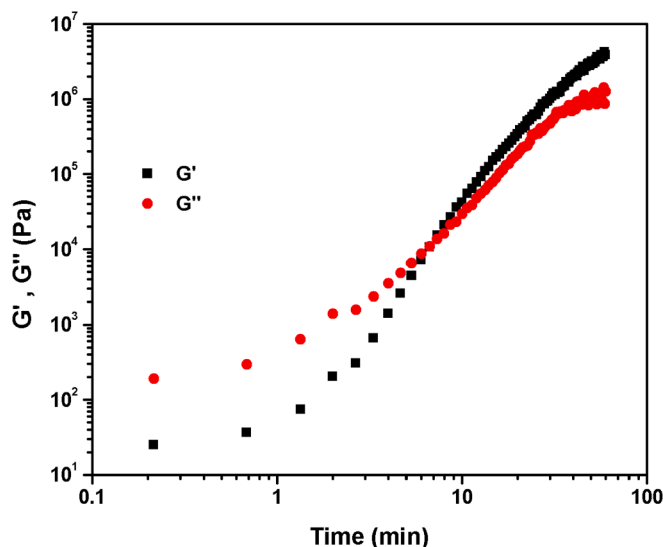


Fig. 6. The evolution of the storage (G') and loss (G'') moduli of *t*-BF-*a*-*c* monomer as a function of time at 160 °C.

The time at which the evolving dynamic storage (G') and loss (G'') moduli intersect during the isothermal polymerization is known as gelation point [28]. The viscoelastic properties of *t*-BF-*a*-*c* benzoxazine monomer against time at 160 °C isothermal polymerization are illustrated as Fig. 6. The *t*-BF-*a*-*c* benzoxazine resin achieves a gelled state in approximately 7 min.

3.3. Thermomechanical and thermal properties

The thermomechanical properties of poly (*t*-BF-*a*-*c*) were evaluated by DMA, the produced results are plotted as Fig. 7. The T_g of poly (*t*-BF-*a*-*c*) was dramatically improved as compared to the bi-functional fluorene-based polybenzoxazine (poly (BF-*p*), 256 °C by DMA; poly (B-*p*bf), 229 °C by DSC [12,15] in spite the incorporation of long alkyl side groups, the T_g was recorded at 373 °C from the $\tan \delta$ peak height. As discussed earlier each *t*-BF-*a*-*c* benzoxazine resin molecule possesses four oxazine rings and olefinic double bonds, resulting in a higher crosslinking density of polybenzoxazine. In the bi-functional fluorene-based polybenzoxazines, the fluorene molecules protrude vertically from the main chain of the polymer. In the current study, the fluorene molecule exists in the backbone of molecule structure, due to this the internal rotations and thermal motions of polymer segments are

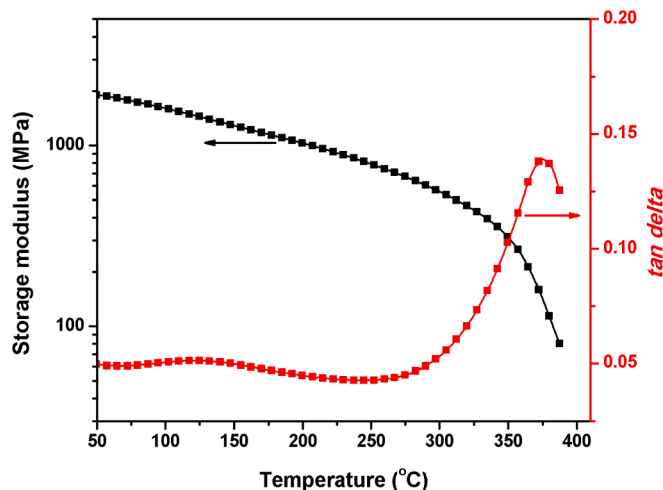


Fig. 7. Storage modulus and loss tangent as a function of temperature for poly (*t*-BF-*a*-*c*).

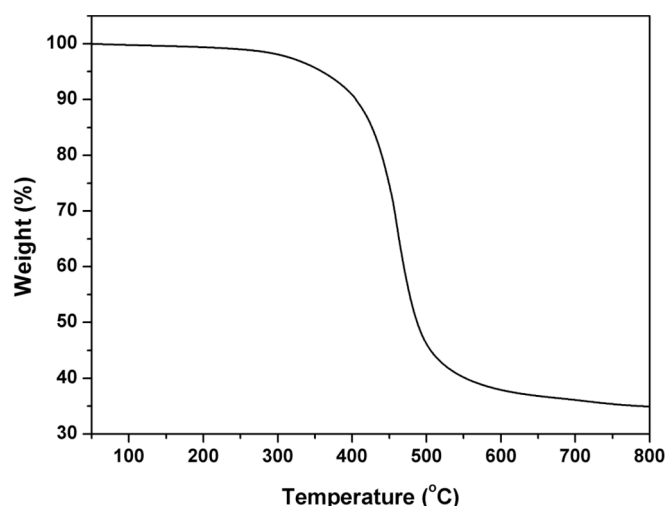


Fig. 8. TGA curve of poly (t-BF-a-c) under a nitrogen atmosphere.

Table 1

Comparison of the glass transition and TGA parameters of poly (t-BF-a-c) with other polybenzoxazine matrices.

Sample	T _g (°C)	T _{5%} (°C)	T _{10%} (°C)	Y _c (% , 800 °C)	Reference
Poly (t-BF-a-c)	373	364	405	35	Current study
Poly (B-pbf)	229	334	364	51	[12]
Poly (BF-p)	256	401	432	49	[15]
Poly (Bzc-A)	104	355	389	12 ^a	[29]
Poly (Bzc-HP)	–	348	377	29 ^a	
Poly (Bzc-HM)	–	354	377	19 ^a	
Poly (Bzc-dds)	–	292	350	12 ^a	
Poly (Bzc-BA)	–	323	374	18 ^a	

^a Y_c recorded at 700 °C.

prevented. However, a significant decline in the stiffness value (storage modulus at 50 °C) was recorded for the poly (t-BF-a-c). The recorded value was about 1.9 GPa, which around 0.7 GPa lower than the stiffness value recorded for poly (BF-p) (2.6 GPa) [15]. This decline in the stiffness value can be devoted to the introduction of a flexible alkyl side chain of Cardanol, which reduced the rigidity of polybenzoxazine and improved the toughness of fluorene-containing polybenzoxazine.

The TGA under a nitrogen atmosphere of poly (t-BF-a-c) was performed to evaluate the thermal stability of polymer, Fig. 8 shows the produced TGA curve. The initial decomposition temperatures corresponding to 5% and 10% weight loss temperatures (T_{5%} and T_{10%}) and char yield (Y_c) at 800 °C are summarized in Table 1.

The initial decomposition temperature values of poly (t-BF-a-c) were recorded as 364 and 405 °C, for the T_{5%} and T_{10%}, respectively. These values are lower than the earlier recorded values for poly (BF-p), but much higher than those of poly (B-pbf) and reported cardanol-based polybenzoxazines. In addition to this, similar behavior was recorded for the Y_c value, the recorded value was 14 and 16% lower than the Y_c value observed for poly (BF-p) and poly (B-pbf), respectively. A 35% Y_c value was recorded for the poly (t-BF-a-c). However, this Y_c value is much higher than the corresponding values recorded in 12–29% range for mono and bi-functional cardanol-based polybenzoxazines [12,15,29]. These enhancements in the thermal stabilities values can be attributed to the high aromatic content and tighter packing density because of the higher crosslinking density for poly (t-BF-a-c). It reflects that cardanol containing tetra-functional fluorene-based polybenzoxazine has excellent processability and thermal stability, and thermomechanical properties. The produced polymer can be an ideal material for electronic packaging materials, laminate materials, and high performance composite substrates.

4. Conclusions

In this work, a novel cardanol containing tetra-functional fluorene-based *t*-BF-a-c benzoxazine having both diamine and bisphenol-type oxazine rings have been successfully prepared. The curing characteristic of *t*-BF-a-c benzoxazine was studied by DSC and FTIR analysis and found similar to di-functional benzoxazine monomers. In addition to this, the *t*-BF-a-c benzoxazine showed better processability. The poly (*t*-BF-a-c) exhibits higher T_g and better thermal stability than those of mono-functional and bi-functional cardanol-based polybenzoxazines due to the rigid backbone. The cross-linking of the polymer was improved due to the cardanol flexible long alkyl groups. The incorporation of flexible long alkyl groups reduced the stiffness of the poly (*t*-BF-a-c), which will have positive impacts on the toughness and mechanical properties without sacrificing thermal properties compared to bi-functional polybenzoxazines.

Acknowledgments

This work is financially sponsored by the National Natural Science Foundation of China, China (Project No.51773048 and 50973022), Natural Science Foundation of Heilongjiang Province, China (Project No. E2017022), and the Open Research Fund of State Key Laboratory of Polymer Physics and Chemistry, Changchun Institute of Applied Chemistry, Chinese Academy of Sciences, China (Project no. 2017-16).

References

- [1] A.-r. Wang, et al., Bio-based phthalonitrile compounds: synthesis, curing behavior, thermomechanical and thermal properties, *React. Funct. Polym.* 127 (2018) 1–9.
- [2] Y.-P. Chen, et al., Synthesis of cardanol-based phthalonitrile monomer and its copolymerization with phenol–aniline-based benzoxazine, *J. Appl. Polym. Sci.* 136 (20) (2019) 47505.
- [3] C. Voirin, et al., Functionalization of cardanol: towards biobased polymers and additives, *Polym. Chem.* 5 (9) (2014) 3142–3162.
- [4] M. Monisha, et al., Cardanol benzoxazines: a versatile monomer with advancing applications, *Macromol. Chem. Phys.* 220 (3) (2019) 1970005.
- [5] A. Devi, D. Srivastava, Studies on the blends of cardanol-based epoxidized novolac type phenolic resin and carboxyl-terminated polybutadiene (CTPB), *I. Mater. Sci. Eng., A* 458 (1) (2007) 336–347.
- [6] B. Kiskan, Adapting benzoxazine chemistry for unconventional applications, *React. Funct. Polym.* 129 (2018) 76–88.
- [7] N.N. Ghosh, B. Kiskan, Y. Yagci, Polybenzoxazines—new high performance thermosetting resins: synthesis and properties, *Prog. Polym. Sci.* 32 (11) (2007) 1344–1391.
- [8] B. Kiskan, N.N. Ghosh, Y. Yagci, Polybenzoxazine-based composites as high-performance materials, *Polym. Int.* 60 (2) (2011) 167–177.
- [9] H. Ishida, P. Froimowicz (Eds.), *Advanced and Emerging Polybenzoxazine Science and Technology*, Elsevier, 2017.
- [10] Y.-L. Liu, et al., Preparation, characterization, and properties of fluorene-containing benzoxazine and its corresponding cross-linked polymer, *J. Polym. Sci. A Polym. Chem.* 48 (18) (2010) 4020–4026.
- [11] J. Wang, et al., Synthesis, curing behavior and thermal properties of fluorene-containing benzoxazines based on linear and branched butylamines, *React. Funct. Polym.* 74 (2014) 22–30.
- [12] J. Wang, et al., Synthesis, curing behavior and thermal properties of fluorene containing benzoxazines, *Eur. Polym. J.* 46 (5) (2010) 1024–1031.
- [13] Y. Lu, et al., Synthesis and curing kinetics of benzoxazine containing fluorene and furan groups, *Thermochim. Acta* 515 (1) (2011) 32–37.
- [14] H.C. Chang, et al., Synthesis of 9,9-bis(4-aminophenyl)fluorene-based benzoxazine and properties of its high-performance thermoset, *J. Polym. Sci. A Polym. Chem.* 50 (11) (2012) 2201–2210.
- [15] J. Wang, et al., Investigation of the polymerization behavior and regioselectivity of fluorene diamine-based benzoxazines, *Macromol. Chem. Phys.* 214 (5) (2013) 617–628.
- [16] T.A. Reddy, M. Srinivasan, Preparation and properties of cardopolymides containing phenoxaphosphine units, *J. Polym. Sci. A Polym. Chem.* 27 (4) (1989) 1419–1424.
- [17] S.-H. Hsiao, C.-T. Li, Synthesis and characterization of new fluorene-based poly (ether imide)s, *J. Polym. Sci. A Polym. Chem.* 37 (10) (1999) 1403–1412.
- [18] P.R. Srinivasan, V. Mahadevan, M. Srinivasan, Preparation and properties of some cardopolymides, *J. Polym. Sci. Polym. Chem. Ed.* 19 (9) (1981) 2275–2285.
- [19] W. Liu, et al., Curing kinetics and properties of epoxy resin–fluorenyl diamine systems, *Polymer* 49 (20) (2008) 4399–4405.
- [20] X.-y. He, et al., Investigation of synthesis, thermal properties and curing kinetics of fluorene diamine-based benzoxazine by using two curing kinetic methods, *Thermochim. Acta* 564 (2013) 51–58.

- [21] X.-y. He, et al., Synthesis, thermal properties and curing kinetics of fluorene diamine-based benzoxazine containing ester groups, *Eur. Polym. J.* 49 (9) (2013) 2759–2768.
- [22] H. Wang, et al., Synthesis of novel furan-containing tetrafunctional fluorene-based benzoxazine monomer and its high performance thermoset, *RSC Adv.* 4 (110) (2014) 64798–64801.
- [23] B.S. Rao, A. Palanisamy, Monofunctional benzoxazine from cardanol for bio-composite applications, *React. Funct. Polym.* 71 (2) (2011) 148–154.
- [24] Y. Cheng, et al., Synthesis and properties of highly cross-linked thermosetting resins of benzocyclobutene-functionalized benzoxazine, *Macromolecules* 45 (10) (2012) 4085–4091.
- [25] Y. Liu, J. Wang, S. Xu, Synthesis and curing kinetics of cardanol-based curing agents for epoxy resin by in situ depolymerization of paraformaldehyde, *J. Polym. Sci. A Polym. Chem.* 52 (4) (2014) 472–480.
- [26] C. Jubsilp, T. Takeichi, S. Rimdusit, Effect of novel benzoxazine reactive diluent on processability and thermomechanical characteristics of bi-functional polybenzoxazine, *J. Appl. Polym. Sci.* 104 (5) (2007) 2928–2938.
- [27] S. Rimdusit, P. Kunopast, I. Dueramae, Thermomechanical properties of arylamine-based benzoxazine resins alloyed with epoxy resin, *Polym. Eng. Sci.* 51 (9) (2011) 1797–1807.
- [28] D.J. Allen, H. Ishida, Effect of phenol substitution on the network structure and properties of linear aliphatic diamine-based benzoxazines, *Polymer* 50 (2) (2009) 613–626.
- [29] B. Lochab, I.K. Varma, J. Bijwe, Cardanol-based bisbenzoxazines: effect of structure on thermal behaviour, *J. Therm. Anal. Calorim.* 107 (2) (2012) 661–668.